Theoretical Study of Solvent Effects on the Platinum-Catalyzed Oxygen Reduction Reaction

ARTICLE *in* JOURNAL OF PHYSICAL CHEMISTRY LETTERS · MARCH 2010

Impact Factor: 7.46 · DOI: 10.1021/jz9003153 · Source: OAI

7 AUTHORS, INCLUDING:

Yi Liu
California Institute of Technology
41 PUBLICATIONS **1,163** CITATIONS
SEE PROFILE

Boris Merinov
California Institute of Technology
19 PUBLICATIONS **527** CITATIONS
SEE PROFILE

William A. Goddard
California Institute of Technology
1,347 PUBLICATIONS **69,067** CITATIONS
SEE PROFILE

THE JOURNAL OF PHYSICAL CHEMISTRY Letters

pubs.acs.org/JPCL

Theoretical Study of Solvent Effects on the Platinum-Catalyzed Oxygen Reduction Reaction

Yao Sha, Ted H. Yu, Yi Liu, Boris V. Merinov,* and William A. Goddard III*

Materials and Process Simulation Center, California Institute of Technology, Pasadena, California 91125

ABSTRACT We report here density functional theory (DFT) studies (PBE) of the reaction intermediates and barriers involved in the oxygen reduction reaction (ORR) on a platinum fuel cell catalyst. Solvent effects were taken into account by applying continuum Poisson−Boltzmann theory to the bound adsorbates and to the transition states of the various reactions on the platinum (111) surface. Our calculations show that the solvent effects change significantly the reaction barriers compared with those in the gas-phase environment (without solvation). The O_2 dissociation barrier decreases from 0.58 to 0.27 eV, whereas the H + O → OH formation barrier increases from 0.73 to 1.09 eV. In the water-solvated phase, OH formation becomes the rate-determining step for both ORR mechanisms, O_2 dissociation and OOH association, proposed earlier for the gas-phase environment. Both mechanisms become significantly less favorable for the platinum catalytic surface in water solvent, suggesting that alternative mechanisms must be considered to describe properly the ORR on the platinum surface.

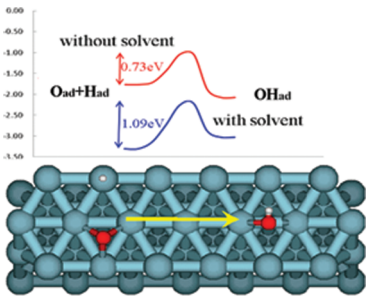

SECTION Surfaces, Interfaces, Catalysis

Polymer electrolyte membrane fuel cells (PEMFCs) have tremendous potential for addressing the world's energy needs but are limited by the efficiency of the cathode catalyst for the oxygen reduction reaction (ORR).[1−4] Currently, the best catalyst is platinum, but it is too expensive and not sufficiently efficient. Many efforts are underway to find replacements or improvements by using different supports, platinum alloys, or nonplatinum catalysts.[5−9] Despite these efforts, there remain uncertainties concerning the fundamental reaction mechanism underlying ORR.

Numerous experimental and theoretical studies have been carried out to study the kinetics of ORR mechanisms.[10−17] Most published theoretical studies simplify the ORR as a reaction in a gas-phase environment, leading to good agreement with the high-vacuum surface experiments on hydrogen oxidation reactions. However, fuel cell operation involves also a solvent environment, and there is not yet a validated efficient method to estimate the contributions of water solvent to the key steps in the reaction mechanisms.

One approach to estimating the solvent effect is to add explicit water molecules (∼4 per unit cell)[11,18] or even an entire water bilayer.[16,17,19] These explicit solvent model approaches lead to plausible results, but the optimum structure for a few waters or a bilayer may not resemble that of the fully solvated system,[20] leading to questions in how to describe the relaxation around the adsorbed species. Moreover, this leads to the possible direct participation of water in the reactions.[21,22] In addition, the periodicity in the solvent structure imposed by the periodic boundary conditions may introduce artificial ordering. Also, without well-justified initial and final configurations, it is difficult to identify the correct solvent structures for transition states to obtain the barriers that determine the reaction rates.

We propose an alternative approach of using the fast but accurate Poisson−Boltzmann implicit continuum model to estimate solvent effects.[23−25] This approach has been applied widely in cluster studies, where it has led to quite accurate results for many systems.[26−28] The contributions of solvent and ions are considered through their electrostatic interactions with the solutes. The use of a continuum solvent environment leads to a consistent model for estimating the contribution of the solvent all along the reaction surface. Details of our approach are given below.

We studied systematically the adsorption preference of six adsorbed intermediates, H (atomic hydrogen), O (atomic oxygen), O_2 (molecular oxygen), OH, OOH, and H_2O on the Pt(111) surface (Table 1), by density function theory (DFT).

All adsorbates prefer one of four binding sites available on the (111) surface (Figure 1), which are denoted as μ_1 (top), μ_2 (bridge), μ_3-fcc (fcc hollow), and μ_3-hcp (hcp hollow), according to the number of surface atoms to which the adsorbate binds.

Without solvation, we find that atomic oxygen (O) prefers the μ_3-fcc site, with a binding energy of BE = 3.68 eV, followed by the μ_3-hcp site with BE = 3.30 eV. This agrees with the experimental adsorption energy of 3.68 eV at the μ_3-fcc adsorption site.[29] Previous theoretical studies on three-layer slabs using the generalized gradient approximation (GGA) of

Received Date: November 25, 2009
Accepted Date: January 26, 2010
Published on Web Date: February 15, 2010

DOI: 10.1021/jz9003153 | J. Phys. Chem. Lett. 2010, 1, 856–861

Table 1. Binding Energies without Solvent (E_{bind}), Slab Charge (Q_{slab}), Solvation Energy (E_{solv}), and Binding Energy with Solvation (E_{bind}^{solv}) for All Intermediates[a]

adsorbate	binding sites	E_{bind} (eV)	Q_{slab}(eV)	E_{solv}(eV)	E_{bind}^{solv} (eV)	$E_{explicit}^{solv}$(eV)
H	μ_1	−2.79	−0.11	−0.07	−2.86	−0.04−0.17[20]
	μ_2	−2.70	−0.21	−0.12	−2.82	
	μ_3-fcc	−2.73	−0.23	−0.12	−2.85	
	μ_3-hcp	−2.70	−0.22	−0.12	−2.82	
O	μ_1	−2.30	0.55	−0.75	−3.05	
	μ_2	−3.11	0.61	−0.63	−3.74	
	μ_3-fcc	−3.68	0.70	−0.70	−4.38	
	μ_3-hcp	−3.30	0.66	−0.63	−3.93	
OH	μ_1	−2.24	0.33	−0.54	−2.78	−0.59[47,48,50]
	μ_2	−2.26	0.25	−0.38	−2.64	
	μ_3-fcc	−1.67	0.34	−0.32	−1.99	
	μ_3-hcp	−1.55	0.34	−0.34	−1.89	
O_2	bridge	−0.41	0.40	−0.32	−0.73	
	fcc	−0.48	0.51	−0.41	−0.89	
	hcp	−0.36	0.47	−0.36	−0.72	
OOH[b]	μ_1-bridge	−1.06	0.26	−0.47	−1.53	
	μ_1-fcc	−0.96	0.27	−0.47	−1.43	
H_2O	μ_1	−0.22	−0.10	−0.36	−0.58	−0.62[49]

[a] E_{bind} is calculated as $E_{slab-adsorbate} - E_{slab} - E_{adsorbate}$. Q_{slab} (e) is the net charge of the slab. E_{solv} (eV) is the solvation energy calculated using the continuum model. E_{bind}^{solv} (eV) is the sum of E_{bind} and E_{bind}^{solv} (eV). [b] Both OOH configurations are atop sites. The only difference is the orientation of OOH.

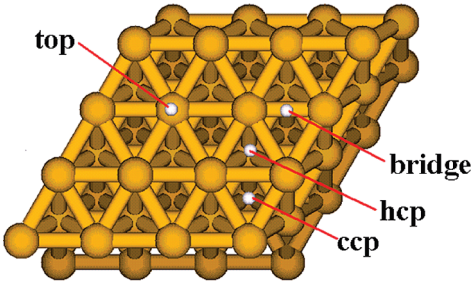

Figure 1. Important binding sites on the closest-packed Pt(111) surface.

Perdew and Wang (PW91) DFT led to BE = 4.03 eV for the μ_3-fcc site.[10] B3LYP DFT calculations on a 35 atom Pt cluster[14] (Pt_{35}) led to BE = 3.37 eV for fcc and 3.03 eV for hcp sites.

Without solvation, we find that O_2 prefers the μ_3-fcc site with BE = 0.48 eV and R_{OO} = 1.41 Å, followed by the μ_2-bridge site with BE = 0.41 eV and R_{OO} = 1.34 Å. This agrees well with low-temperature adsorption experiments[30] that find that O_2 can absorb into both a peroxide-like (O_2^{2-}) with a vibrational frequency of 690 cm^{-1} and a weaker bound superoxo-like (O_2^{-}) with a vibrational frequency of 870 cm^{-1}. Our bond lengths agree with experimental estimates of 1.43 Å for peroxo-like and 1.37 Å for superoxo-like species.[31] Our calculated BE is consistent with the experimental estimate of 0.38 eV for the superoxo-like configuration.[32] Earlier theoretical studies[12,33] led to 0.65−0.72 eV for peroxo-like and 0.53−0.68 eV for superoxo-like. This difference is mainly due to the smaller number of layers included in these earlier studies. Thus, we find that using only three-layer slabs, as in the previous studies, leads to 0.62 and 0.75 eV, respectively. B3LYP DFT calculations on a 35 atom Pt cluster[14] found the bridge site to be preferred with BE = 0.49 eV, while calculations on a 5 atom cluster[34] led to BE = 0.53 eV for the bridge site.

We find that OH prefers the μ_2 (bridge) site with BE = 2.26 eV, while the μ_1 site is close with BE = 2.24 eV. This agrees with the calculations on a three-layer slab using GGA PW91 DFT by Hu,[35] who found BE = 2.22 eV for the μ_2 (bridge) site and 2.27 eV for the μ_1 site. B3LYP calculations for the Pt_{35} cluster[14] obtained BE = 2.06 eV. It is important to note that this OH structure would not be stable for a monolayer, which would reconstruct into an overlayer having a network of hydrogen bonds.[35] Here, we use this structure just to estimate the solvation energy (without considering stabilization from adjacent OH).

We find that OOH is stable only on the μ_1 (top) site, leading to an optimum configuration in which the O−O bond is parallel to the surface pointing toward an adjacent Pt atom, leading to BE = 1.06 eV. An alternative configuration for OOH has the O−O bond pointing toward an adjacent fcc site with a BE of 0.96 eV. This implies 0.08 eV agostic stabilization from the adjacent surface atom. Similar results were obtained for the Pt_{35} cluster[14] with BE = 1.03 eV.

We find that H_2O is stable only on the atop site, with a binding energy of 0.22 eV without solvent. This agrees with 0.29 eV for the atop site in three-layer calculations using PBE studies.[36] Calculations for the Pt_{35} cluster led to a much stronger BE = 0.61 eV. Direct comparison with experiment is difficult since H_2O tends to form a bilayer.[19,36]

Our PBE calculations find that the μ_1 (BE = 2.79 eV) and μ_3-fcc (BE = 2.73 eV) sites are most stable for atomic hydrogen (Table 1). This result agrees with the high-resolution

DOI: 10.1021/jz9003153 | J. Phys. Chem. Lett. 2010, 1, 856–861

Table 2. Reaction Barriers without Solvent (E_a) and in the Water-Solvated Phase (E_a^{solv}) for Five Steps Involved in the O_2 Dissociation and OOH Association Pathways

barriers	reaction steps	E_a (eV)	E_a^{solv} (eV)
barriers for steps	O_2 dissociation	0.58	0.27
	OH formation	0.73	1.09
	H_2O formation	0.21	0.33
	OOH formation	0.31	0.28
	OOH dissociation	0.17	0.00
barriers for the overall reaction	O_2 dissociation	0.73	1.09
	OOH dissociation	0.73	1.09

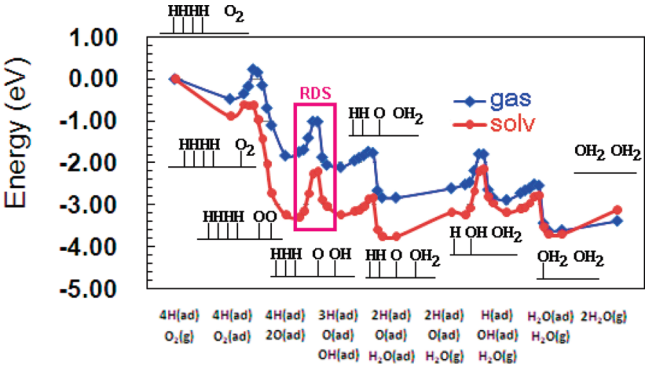

Figure 2. Potential energy surface of the O_2 dissociation mechanism without and with water solvent.

electron energy loss spectroscopy (HREELS) experiment,[37] which found H in the three-fold-coordinated site, and with vibrational neutron spectroscopy studies,[38] where hydrogen was observed in the on-top site. Our calculations for the six-layer slab find that atomic hydrogen slightly prefers the on-top site over the three-fold-coordinated site by 0.06 eV (0.02 eV after zero-point energy correction). This is consistent with the small experimental hydrogen diffusion barrier of ~0.07 eV.[39] For such small differences, one must consider the biases in the particular form of DFT; indeed, Olsen et al.[40] showed that various exchange−correlation functional can change binding energies by up to 0.1 eV, setting a bound on the accuracy to be expected from such studies.

Two reaction pathways were proposed previously[14] for the ORR on the Pt(111) metal surface in the gas-phase environment, the O_2 dissociation mechanism

$$O_2 \underset{i}{\rightarrow} 2O \overset{2H}{\underset{ii}{\rightarrow}} 2OH \overset{2H}{\underset{iii}{\rightarrow}} 2H_2O \qquad (1)$$

and the OOH association mechanism

$$O_2 \overset{H}{\underset{iv}{\rightarrow}} OOH \underset{v}{\rightarrow} O + OH \overset{H}{\underset{ii}{\rightarrow}} 2OH \overset{2H}{\underset{iii}{\rightarrow}} 2H_2O \qquad (2)$$

where all reactants are surface adsorbates describing the hydrogen oxidation reaction after dissociative adsorption of H_2. Both of these mechanisms are supported by subsequent calculations.[11,41]

We computed transition states and barriers using nudged elastic band theory (NEB)[42,43] for all five reaction steps (i−v) involved in pathways 1 and 2. The results are shown in Table 2 and Figures 2 and 3.

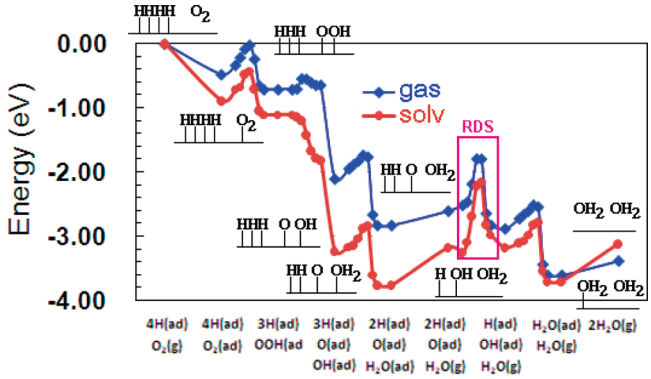

Figure 3. Potential energy surface of the OOH association mechanism without and with water solvent.

The three barriers in the O_2 dissociation mechanism (pathway 1) in the gas-phase environment were calculated to be 0.58 eV for O_2 dissociation, 0.73 eV for OH formation, and 0.21 eV for H_2O formation (using six-layer slabs). This can be compared with 0.52, 0.91, and 0.14 eV in DFT studies by Li et al.[12] using four layers and with 0.94 and 0.21 eV obtained by Hu[10] for OH and H_2O formation using three-layer slabs. To validate that these differences are due to slab thickness effect, we carried out similar calculations with just a three-layer slab, leading to 0.52, 0.83, and 0.25 eV, which agrees well with previous results. For the Pt_{35} cluster,[14] the barriers were 0.63, 1.13, and 0.09 eV.

For the OOH association mechanism (pathway 2), we found the barriers of 0.31 eV for OOH formation, 0.17 eV for OOH dissociation, 0.73 eV for OH formation, and 0.21 eV for H_2O formation, all with six-layer slabs. Using only three layers, we found the OOH to be 0.37 eV, which agrees with the 0.42 eV calculated by Li[12] for three layers. Again, we found OH formation to be the rate-determining step (RDS) in the OOH association mechanism.

Summarizing, our calculations predict that the ORR on the Pt(111) surface in the gas-phase environment would have a total energy barrier of 0.73 eV, with the OH formation as the RDS for both the O_2 dissociation and OOH association mechanisms.

The solvent effects on all adsorbed species, ORR intermediates, and transition states were evaluated using the adaptive Poisson−Boltzmann solver (APBS) method[44−46] at single points using the structures optimized in the gas phase. Energies and potential energy surfaces including the solvent effects as described in eq 3 are shown in Tables 1 and 2 and Figures 2 and 3.

Table 1 shows that the solvation energy for adsorbed OH (top) is 0.54 eV, which agrees with the first-layer solvation energy of 0.54 eV estimated for an adsorbed OH/H_2O overlayer.[47] This becomes an overall solvation of 0.59 eV after including the second-layer solvation energy of 0.05 eV due to wetting of the OH/H_2O overlayer.[48]

We find that solvation stabilizes the water molecule by 0.36 eV, giving a total binding energy of 0.58 eV. This agrees with 0.62 eV from extensive calculations of water adsorption by Meng et al.[49] using up to six bilayers of explicit water.

The solvation energy for adsorbed hydrogen is only 0.07 (μ_1) or 0.12 (μ_3) eV for six layers, reflecting the similar

DOI: 10.1021/jz9003153 | J. Phys. Chem. Lett. 2010, 1, 856–861

electronegativity of H and Pt. This agrees with the range of 0.04−0.17 eV from studies of surface hydrogen using an explicit solvation method.[20]

We find that the solvent strongly stabilizes adsorbed oxygen by 0.63−0.75 eV, whereas adsorbed O_2 (fcc) is stabilized by 0.41 eV and OOH is stabilized by 0.47 eV. Our calculated solvation of adsorbed O does not agree with the estimate of −0.03 eV by Norskov[50] using the water bilayer, who assumed that the O would not change the structure of the water bilayer (no details were provided).

Summarizing, we find that solvent effects significantly modify the reaction energies and ORR barriers for both mechanisms.

For the direct O_2 dissociation mechanism, the barriers for the three steps, O_2 dissociation, OH formation, and H_2O formation, are estimated to change by −0.31, 0.36, and 0.12 eV, respectively, in the presence of water.

For the OOH association mechanism, solvation changes the barriers for the four steps, OOH formation, OOH dissociation, OH formation, and H_2O formation, by −0.03, −0.17, 0.36, and 0.12 eV, respectively.

With solvation, the RDS for both mechanisms becomes the OH formation step, with a barrier of 1.09 eV in water solvent. Such a high barrier would seem to provide rates at the operating temperature of a PEMFC (below 90 °C) that are too low. This makes it questionable whether either of the two reaction mechanisms considered above can be responsible for the rates in water solvent. Thus, one of the following will occur.

- The chemistry must occur through surface structures different than (111) on Pt (perhaps steps)
- The OH formation and H_2O formation steps in ORR must be assumed to occur mainly through a hydronium-induced mechanism.[16,17] As discussed above, we assume that the hydrogen involved in various reaction steps is already on the surface. This assumption is based on the observation that hydrogen is easily adsorbed on the surface with a small energy barrier of 0.15 eV in the presence of the water bilayer.[51] In PEMFCs, H_3O^+ stabilized by the sulfonates of the Nafion could serve as a source of hydrogen[11] for formation of OH from O_{ad} (and possibly for forming OOH and H_2O), but consideration of H_3O^+ is beyond the scope of this publication.
- Some other mechanism might exist for the ORR on the platinum surface.

Our slab calculations of the ORR on the Pt(111) surface were performed with the SEQQUEST DFT code[52] using the Perdew−Becke−Ernzerhof (PBE)[53] exchange−correlation functional of the generalized gradient approximation (GGA).[54,55] SEQQUEST uses local Gaussian-type basis functions (double-ζ plus polarization quality, optimized for bulk systems) rather than periodic plane waves. In SEQQUEST, the Kohn−Sham equations[56] are solved self-consistently using two-dimensional periodic conditions. The 62 core electrons ($Kr[5s^24d^{10}4f^{14}]$) of platinum are replaced with an angular momentum projected[57,58] norm-conserving[59,60] effective core potential (ECP) so that only 16 electrons are considered explicitly. The real space grid density is 7 points/Å.

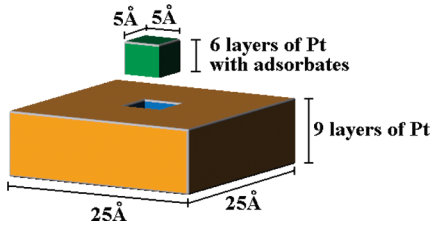

Figure 4. The super slab used to calculate the solvent effect. Only the center cell has adsorbate attached. All cells surrounding the center cell contain neutral platinum atoms. Three additional layers of platinum are added to the bulk side to eliminate extraneous solvent effects.

The active Pt(111) surface was modeled using a metal slab that is infinitely periodic along two dimensions but finite along the third one. We used a 2 × 2 hexagonal unit cell with four metal atoms per layer and six layers in total to model the catalyst. All calculations were performed with the optimized cell parameter of 3.98 Å found in the bulk calculation using the PBE DFT. We allowed the atoms in the top two layers to relax to their lowest-energy configuration while fixing the atoms of the bottom four layers to their bulk positions. All binding configurations and transition states were determined using PBE DFT calculations without solvation. Then, we carried out single-point calculations to include the solvent effect. The total energy was represented as the sum of gas-phase and solvation energies

$$E_{total} = E_{gas} + E_{solv} \quad (3)$$

We evaluated the solvent effect using the Poisson−Boltzmann implicit solvent method as implemented in the APBS,[44−46] which is incorporated in the Computational Materials Design Facility[61] (CMDF) developed in the Materials and Process Simulation Center (MSC) at Caltech. Here, the boundary of the continuum is taken as the solvent-accessible surface for a solvent with a spherical radius of 1.4 Å and a dielectric constant of 78. Structures and charges were taken from PBE for all intermediates and transition states. To test whether more than 6 layers might be needed, we carried out calculations for 3−10 layers and found negligible energy changes (~0.02 eV) between 6 and 10 layers.

However, we were concerned that calculations of the solvent effect might require larger slabs since the electrostatic interaction between the solvent and solute may converge slowly. Thus, we used an alternative approach to evaluate the solvent effect. Here, instead of solving the Poisson−Boltzmann equation for a periodic system, we cut a super cell out of the infinite pure platinum slab. The center cell was substituted by the adsorbing system of interest, while all remaining cells were similar to those in the original platinum slab. Thus, a center cell with adsorbate was surrounded by bare and hence neutral ones. To avoid solvent stabilization due to interaction between the solvent and the back side of the slab (the bulk side), we added three additional layers of neutral platinum atoms to the bulk side. A sketch of the model is shown in Figure 4.

Summarizing, we report the structures, binding energies, and reaction barriers from PBE DFT studies of the reaction intermediates involved in ORR on platinum slabs containing

DOI: 10.1021/jz9003153 | J. Phys. Chem. Lett. 2010, 1, 856–861

six layers of Pt. These calculations use the Poisson–Boltzmann method to include the effects of solvation. We considered two previously proposed mechanisms (O_2 dissociation and OOH association) and found that the energetics of the ORR on the Pt surface changed significantly in the presence of water solvent. In particular, the OH formation was found to be the RDS for both mechanisms, leading to an overall energy barrier increase to 1.09 eV in the solvent, compared to 0.73 eV without solvation. With such a high barrier in the solvent, these two gas-phase ORR mechanisms became unfavorable and we conclude that the chemistry must occur through surface structures different than (111) (e.g., steps) or the ORR must be assumed to involve a hydronium-induced mechanism or another mechanism must exist for the ORR on the platinum surface.

AUTHOR INFORMATION

Corresponding Author:

*To whom correspondence should be addressed. Fax: +1 626 585 0918. E-mail: merinov@wag.caltech.edu (B.V.M.); wag@wag.caltech.edu (W.A.G.).

ACKNOWLEDGMENT This work was supported partially by the U.S. Department of Energy under Grant DE-AC02-06CH11357 and partially by Ford Motor Company (Dr. Pezhman Shirvanian). The facilities of the MSC used in this study were established with grants from DURIP-ONR and DURIP-ARO.

REFERENCES

(1) Kordesch, K.; Simader, G. *Fuel Cells and Their Applications*; VCH: New York, 1996.
(2) Appleby, A.; Foulkes, F. *Fuel Cell Handbook*; Van Nostrand Reinhold: New York, 1989.
(3) Brandon, N. P.; Skinner, S.; Steele, B. C. H. Recent Advances in Materials for Fuel Cells. *Ann. Rev. Mater. Res.* **2003,** *33*, 183–213.
(4) Mehta, V.; Cooper, J. S. Review and Analysis of PEM Fuel Cell Design and Manufacturing. *J. Power Sources* **2003,** *114*, 32–53.
(5) Baturina, O. A.; Garsany, Y.; Zega, T. J.; Stroud, R. M.; Schull, T.; Swider-Lyons, K. E. Oxygen Reduction Reaction on Platinum/Tantalum Oxide Electrocatalysts for PEM Fuel Cells. *J. Electrochem. Soc.* **2008,** *155*, B1314–B1321.
(6) Neophytides, S.; Murase, K.; Zafeiratos, S.; Papakonstantinou, G.; Paloukis, F.; Krstajic, N.; Jaksic, M. Composite Hypo-Hyper-d-Intermetallic and Interionic Phases As Supported Interactive Electrocatalysts. *J. Phys. Chem. B* **2006,** *110*, 3030–3042.
(7) Shim, J.; Lee, C. R.; Lee, H. K.; Lee, J. S.; Cairns, E. J. Electrochemical Characteristics of Pt-WO3/C and Pt-TiO2/C Electrocatalysts in a Polymer Electrolyte Fuel Cell. *J. Power Sources* **2001,** *102*, 172–177.
(8) Xiong, L.; Manthiram, A. Synthesis and Characterization of Methanol Tolerant Pt/TiOx/C Nanocomposites for Oxygen Reduction in Direct Methanol Fuel Cells. *Electrochim. Acta* **2004,** *49*, 4163–4170.
(9) Wang, B. Recent Development of Non-platinum Catalysts for Oxygen Reduction Reaction. *J. Power Sources* **2005,** *152*, 1–15.
(10) Michaelides, A.; Hu, P. Catalytic Water Formation on Platinum: A First-Principles Study. *J. Am. Chem. Soc.* **2001,** *123*, 4235–4242.
(11) Hyman, M. P.; Medlin, J. W. Mechanistic Study of the Electrochemical Oxygen Reduction Reaction on Pt(111) Using Density Functional Theory. *J. Phys. Chem. B* **2006,** *110*, 15338–15344.
(12) Qi, L.; Yu, J. G.; Li, J. Coverage Dependence and Hydroperoxyl-Mediated Pathway of Catalytic Water Formation on Pt(111) Surface. *J. Chem. Phys.* **2006,** *125*, 8.
(13) Zhang, T.; Anderson, A. B. Oxygen Reduction on Platinum Electrodes in Base: Theoretical Study. *Electrochim. Acta* **2007,** *53*, 982–989.
(14) Jacob, T.; Goddard, W. A. Water Formation on Pt and Pt-Based Alloys: A Theoretical Description of a Catalytic Reaction. *ChemPhysChem* **2006,** *7*, 992–1005.
(15) Nilekar, A. U.; Mavrikakis, M. Improved Oxygen Reduction Reactivity of Platinum Monolayers on Transition Metal Surfaces. *Surf. Sci.* **2008,** *602*, L89–L94.
(16) Janik, M. J.; Taylor, C. D.; Neurock, M. First-Principles Analysis of the Initial Electroreduction Steps of Oxygen over Pt(111). *J. Electrochem. Soc.* **2009,** *156*, B126–B135.
(17) Norskov, J. K.; Rossmeisl, J.; Logadottir, A.; Lindqvist, L.; Kitchin, J. R.; Bligaard, T.; Jonsson, H. Origin of the Overpotential for Oxygen Reduction at a Fuel-Cell Cathode. *J. Phys. Chem. B* **2004,** *108*, 17886–17892.
(18) Wang, Y.; Balbuena, P. Ab Initio Molecular Dynamics Simulations of the Oxygen Reduction Reaction on a Pt(111) Surface in the Presence of Hydrated Hydronium $(H_3O)+(H_2O)_2$: Direct or Series Pathway? *J. Phys. Chem. B* **2005,** *109*, 14896–14907.
(19) Ogasawara, H.; Brena, B.; Nordlund, D.; Nyberg, M.; Pelmenschikov, A.; Pettersson, L.; Nilsson, A. Structure and Bonding of Water on Pt(111). *Phys. Rev. Lett.* **2002,** *89*, 276102.
(20) Hamada, I.; Morikawa, Y. Density-Functional Analysis of Hydrogen on Pt(111): Electric Field, Solvent, And Coverage Effects. *J. Phys. Chem. C* **2008,** *112*, 10889–10898.
(21) Xu, X.; Muller, R. P.; Goddard, W. A. The Gas Phase Reaction of Singlet Dioxygen with Water: A Water-Catalyzed Mechanism. *Proc. Natl. Acad. Sci. U.S.A.* **2002,** *99*, 3376–3381.
(22) Keith, J. A.; Oxgaard, J.; Goddard, W. A. Inaccessibility of β-Hydride Elimination from −OH Functional Groups in Wacker-Type Oxidation. *J. Am. Chem. Soc.* **2006,** *128*, 3132–3133.
(23) Tomasi, J.; Persico, M. Molecular Interactions in Solution: An Overview of Methods Based on Continuous Distributions of the Solvent. *Chem. Rev.* **1994,** *94*, 2027–2094.
(24) Cramer, C.; Truhlar, D. Implicit Solvation Models: Equilibria, Structure, Spectra, And Dynamics. *Chem. Rev.* **1999,** *99*, 2161–2200.
(25) Tannor, D. J.; Marten, B.; Murphy, R.; Friesner, R. A.; Sitkoff, D.; Nicholls, A.; Ringnalda, M.; Goddard, W. A., III; Honig, B. Accurate First Principles Calculation of Molecular Charge Distributions and Solvation Energies from Ab Initio Quantum Mechanics and Continuum Dielectric Theory. *J. Am. Chem. Soc.* **1994,** *116*, 11875–11882.
(26) Rogstad, K. N.; Jang, Y. H.; Sowers, L. C.; Goddard, W. A. First Principles Calculations of the pK_a Values and Tautomers of Isoguanine and Xanthine. *Chem. Res. Toxicol.* **2003,** *16*, 1455–1462.
(27) Nielsen, R. J.; Goddard, W. A. Mechanism of the Aerobic Oxidation of Alcohols by Palladium Complexes of *N*-Heterocyclic Carbenes. *J. Am. Chem. Soc.* **2006,** *128*, 9651–9660.

DOI: 10.1021/jz9003153 | *J. Phys. Chem. Lett.* **2010,** *1*, 856–861

(28) Jones, C. J.; Doug, T.; Ziatdinov, V. R.; Periana, R. A.; Nielsen, R. J.; Oxgaard, J.; Goddard, W. A. Selective Oxidation of Methane to Methanol Catalyzed, with C−H Activation, by Homogeneous, Cationic Gold. *Angew. Chem., Int. Ed.* **2005,** *43*, 2–5.
(29) Parker, D.; Bartram, M.; Koel, B. Study of High Coverages of Atomic Oxygen on the Pt(111) Surface. *Surf. Sci.* **1989,** *217*, 489–510.
(30) Nolan, P.; Lutz, B.; Tanaka, P.; Davis, J.; Mullins, C. Translational Energy Selection of Molecular Precursors to Oxygen Adsorption on Pt(111). *Phys. Rev. Lett.* **1998,** *81*, 3179–3182.
(31) Puglia, C.; Nilsson, A.; Hernnas, B.; Karis, O.; Bennich, P.; Martensson, N. Physisorbed, Chemisorbed and Dissociated O_2 on Pt(111) Studied by Different Core-Level Spectroscopy Methods. *Surf. Sci.* **1995,** *342*, 119–133.
(32) Gland, J. L.; Sexton, B. A.; Fisher, G. B. Oxygen Interactions with the Pt(111) Surface. *Surf. Sci.* **1980,** *95*, 587–602.
(33) Eichler, A.; Hafner, J. Molecular Precursors in the Dissociative Adsorption of O_2 on Pt(111). *Phys. Rev. Lett.* **1997,** *79*, 4481–4484.
(34) Li, T.; Balbuena, P. B. Oxygen Reduction on a Platinum Cluster. *Chem. Phys. Lett.* **2003,** *367*, 439–447.
(35) Michaelides, A.; Hu, P. A Density Functional Theory Study of Hydroxyl and the Intermediate in the Water Formation Reaction on Pt. *J. Chem. Phys.* **2001,** *114*, 513–519.
(36) Meng, S.; Xu, L. F.; Wang, E. G.; Gao, S. W. Vibrational Recognition of Hydrogen-Bonded Water Networks on a Metal Surface. *Phys. Rev. Lett.* **2002,** *89*, 176101.
(37) Badescu, C.; Salo, P.; Ala-Nissila, T.; Ying, S.; Jacobi, K.; Wang, Y.; Bedürftig, K.; Ertl, G. Energetics and Vibrational States for Hydrogen on Pt(111). *Phys. Rev. Lett.* **2002,** *88*, 136101.
(38) Parker, S. F.; Frost, C. D.; Telling, M.; Albers, P.; Lopez, M.; Seitz, K. Characterisation of the Adsorption Sites of Hydrogen on Pt/C Fuel Cell Catalysts. *Catal. Today* **2006,** *114*, 418–421.
(39) Graham, A. P.; Menzel, A.; Toennies, J. P. Quasielastic Helium Atom Scattering Measurements of Microscopic Diffusional Dynamics of H and D on the Pt(111) Surface. *J. Chem. Phys.* **1999,** *111*, 1676–1685.
(40) Olsen, R.; Kroes, G.; Baerends, E. Atomic and Molecular Hydrogen Interacting with Pt(111). *J. Chem. Phys.* **1999,** *111*, 11155–11163.
(41) Walch, S.; Dhanda, A.; Aryanpour, M.; Pitsch, H. Mechanism of Molecular Oxygen Reduction at the Cathode of a PEM Fuel Cell: Non-Electrochemical Reactions on Catalytic Pt Particles. *J. Phys. Chem. C* **2008,** *112*, 8464–8475.
(42) Mills, G.; Jonsson, H.; Schenter, G. K. Reversible Work Transition-State Theory — Application to Dissociative Adsorption of Hydrogen. *Surf. Sci.* **1995,** *324*, 305–337.
(43) Mills, G.; Jonsson, H. Quantum and Thermal Effects in H_2 Dissociative Adsorption: Evaluation of Free-Energy Barriers in Multidimensional Quantum Systems. *Phys. Rev. Lett.* **1994,** *72*, 1124–1127.
(44) Baker, N.; Sept, D.; Joseph, S.; Holst, M.; McCammon, J. Electrostatics of Nanosystems: Application to Microtubules and the Ribosome. *Proc. Natl. Acad. Sci. U.S.A.* **2001,** *98*, 10037–10041.
(45) Holst, M.; Saied, F. Multigrid Solution of the Poisson−Boltzmann Equation. *J. Comput. Chem.* **1993,** *14*, 105–113.
(46) Holst, M.; Saied, F. Numerical Solution of the Nonlinear Poisson−Boltzmann Equation: Developing More Robust and Efficient Methods. *J. Comput. Chem.* **1995,** *16*, 337–364.
(47) Karlberg, G. S.; Olsson, F. E.; Persson, M.; Wahnstrom, G. Energetics, Vibrational Spectrum, And Scanning Tunneling Microscopy Images for the Intermediate in Water Production Reaction on Pt(111) from Density Functional Calculations. *J. Chem. Phys.* **2003,** *119*, 4865–4872.
(48) Zimbitas, G.; Gallagher, M. E.; Darling, G. R.; Hodgson, A. Wetting of Mixed OH/H_2O Layers on Pt(111). *J. Chem. Phys.* **2008,** *128*, 12.
(49) Meng, S.; Wang, E. G.; Gao, S. W. Water Adsorption on Metal Surfaces: A General Picture from Density Functional Theory Studies. *Phys. Rev. B* **2004,** *69*, 195404.
(50) Rossmeisl, J.; Norskov, J. K.; Taylor, C. D.; Janik, M. J.; Neurock, M. Calculated Phase Diagrams for the Electrochemical Oxidation and Reduction of Water over Pt(111). *J. Phys. Chem. B* **2006,** *110*, 21833–21839.
(51) Skulason, E.; Karlberg, G. S.; Rossmeisl, J.; Bligaard, T.; Greeley, J.; Jonsson, H.; Norskov, J. K. Density Functional Theory Calculations for the Hydrogen Evolution Reaction in an Electrochemical Double Layer on the Pt(111) Electrode. *Phys. Chem. Chem. Phys.* **2007,** *9*, 3241–3250.
(52) Schultz, P. *SeqQuest Code Project*. Sandia National Laboratories; http://www.cs.sandia.gov/~paschul/Quest/ (2009).
(53) Perdew, J.; Burke, K.; Ernzerhof, M. Generalized Gradient Approximation Made Simple. *Phys. Rev. Lett.* **1996,** *77*, 3865–3868.
(54) Ceperley, D. M.; Alder, B. J. Ground-State of the Electron-Gas by a Stochastic Method. *Phys. Rev. Lett.* **1980,** *45*, 566–569.
(55) Perdew, J. P.; Zunger, A. Self-Interaction Correction to Density-Functional Approximations for Many-Electron Systems. *Phys. Rev. B* **1981,** *23*, 5048–5079.
(56) Kohn, W.; Sham, L. Self-Consistent Equations Including Exchange and Correlation Effects. *Phys. Rev.* **1965,** *140*, A1133–A1138.
(57) Melius, C. F.; Goddard, W. A. Ab-Initio Effective Potentials for Use in Molecular Quantum-Mechanics. *Phys. Rev. A* **1974,** *10*, 1528–1540.
(58) Melius, C. F.; Olafson, B. D.; Goddard, W. A. Fe and Ni Ab-Initio Effective Potentials for Use in Molecular Calculations. *Chem. Phys. Lett.* **1974,** *28*, 457–462.
(59) Redondo, A.; Goddard, W. A.; Mcgill, T. C. Ab initio Effective Potentials for Silicon. *Phys. Rev. B* **1977,** *15*, 5038–5048.
(60) Hamann, D. R. Generalized Norm-Conserving Pseudopotentials. *Phys. Rev. B* **1989,** *40*, 2980.
(61) Goddard, W. A., III; Jaramillo-Botero, A.; Liu, Y.; Duin, A. v.; Buehler, M.; Meulbroek, P.; Dodson, J. *The Computational Materials Design Facility* (*CMDF*) *Project*. http://www.wag.caltech.edu/multiscale/multsicale_computations.htm (2007).

DOI: 10.1021/jz9003153 | *J. Phys. Chem. Lett.* **2010,** *1*, 856–861